



146
162
THS

AN APPARATUS DESIGNED FOR A STUDY OF
THE MEAN LIFE OF THE 129-KEV NUCLEAR
ENERGY STATE OF IR 191

Thesis for the Degree of M. S.
MICHIGAN STATE UNIVERSITY

Ronald Ames Hill

1958

MICHIGAN STATE UNIVERSITY LIBRARIES



3 1293 01687 5902

THESIS

**AN APPARATUS DESIGNED FOR A STUDY OF THE MEAN LIFE
OF THE 129-KEV NUCLEAR ENERGY STATE OF IR 191**

By

RONALD AMES HILL

A THESIS

**Submitted to the College of Science and Arts of
Michigan State university of Agriculture and
Applied Science in partial fulfillment of
the requirements for the degree of**

MASTER OF SCIENCE

Department of Physics

(1958)

RONALD AMES HILL

ABSTRACT

An apparatus is described which is to be used in the determination of the mean life of the 129-kev gamma transition in iridium 191 by nuclear resonance fluorescence.

The apparatus consists of a magnetically suspended, magnetically driven, high speed rotor upon which a source of iridium 191 gamma rays (^{191}Ir) is to be attached in order that the resonance condition be restored through the Doppler effect. A gating system is employed to turn on a scintillation counter when the source is approaching the scatterer to improve the signal to noise ratio.

Peripheral velocities of the order of 4×10^4 cm/sec for a one inch diameter steel rotor have been obtained, well above the 2.2×10^4 cm/sec required for the ^{191}Ir experiment. A test of the gating circuit indicates that the scintillation counter is turned on for a larger portion of the rotor's cycle for faster rotor velocities. This effect will need to be compensated for in the ^{191}Ir experiment.

ACKNOWLEDGEMENTS

I wish to express my sincere appreciation to Dr. W. H. Kelly and Dr. G. B. Beard for their help and encouragement during the progress of this work.

I am grateful to Dr. H. Bendler for his help and suggestions in the development of the apparatus and to Mr. W. Chapman of the General Motors Technical Center for his assistance in the design of the apparatus and for the drive coils so kindly furnished. I wish to thank Mr. W. Perkins of New Departure for furnishing the steel ball bearings, the Messrs. C. Kingston, R. Hoskins and R. Salemka for their help and suggestions in the construction of the apparatus, and the Air Force Office of Scientific Research and the Physics Department of Michigan State University for making this work financially possible through a research assistantship.

TABLE OF CONTENTS

	Page
INTRODUCTION	1
MAGNETICALLY SUSPENDED ROTOR AND ASSOCIATED APPARATUS	9
Historical	9
Magnetic Suspension Apparatus	10
Magnetic Drive Circuit	13
The Rotor	15
Nuclear Counting Equipment	15
PERFORMANCE OF THE APPARATUS	22
Magnetic Suspension system	22
Magnetic Drive Circuit	24
Nuclear Counting Equipment	25
APPENDIX	27
BIBLIOGRAPHY	28

LIST OF FIGURES

Figure:	Page:
1. Decay Scheme of Os 191.	2
2. Magnetic Suspension Apparatus.	11
3. Magnetic Suspension Circuit.	12
4. Magnetic Driving Circuit.	14
5. Photomultiplier Arrangement.	16
6.(a) Block Diagram of Detection System.	19
(b) 931A Pre-Amplifier Circuit.	20
(c) Gate Circuit.	21
7. Gate Width as a Function of Rotor Frequency.	26

INTRODUCTION

The investigation of electromagnetic transitions between nuclear states together with theoretical calculations on internal conversion coefficients, angular correlation and Coulomb excitation have provided much useful data for the study of the properties of nuclear energy levels. Some of the quantities characterizing these nuclear states are energy, total angular momentum, parity, magnetic moment, electric quadrupole moment, partial level widths, and mean lifetimes of excited states. Of particular interest in this investigation is the apparatus to be used in the determination of the mean lifetime of the 129-keV gamma transition in iridium 191 by nuclear resonance fluorescence.

Resonant scattering of gamma rays can occur when an incident photon has an energy corresponding to the energy difference between the ground state and an excited energy level of the scattering nucleus. In the experiment under consideration, one uses a radioactive source decaying to the element under study as the source of the exciting radiation. This is accomplished by using osmium 191 which decays by β^- emission to iridium 191 in the excited state as shown in figure 1.

2.

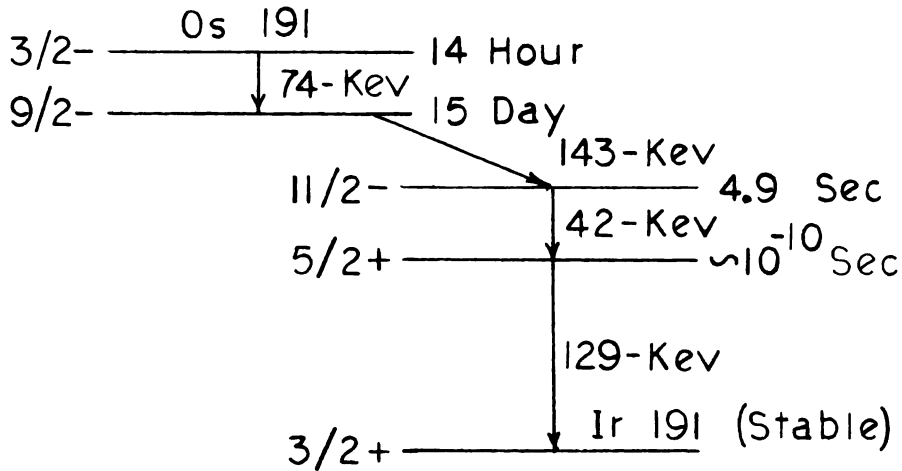


Fig. 1: Decay scheme of Os 191¹.

However, due to the recoil of the decaying nucleus, the energy of the emitted radiation is less than the energy difference between the two levels corresponding to the transition. If E is the energy of the emitted radiation, E_n the energy of the recoiling nucleus and E_0 the energy of the excitation level, then by energy conservation

$$E = h\nu = E_0 - E_n \quad (1)$$

where h is Planck's constant and ν the frequency of the radiation. Now by the conservation of momentum,

$$E_n = \frac{p_n^2}{2m} = \frac{p_\gamma^2}{2m} = \frac{(h\nu)^2}{2mc^2} = \frac{E^2}{2mc^2} \quad (2)$$

where $p_n = p_\gamma$ are the momenta of the recoil nucleus and gamma ray respectively and m is the mass of the emitting nucleus. Combining equations (1) and (2) one obtains

$$h\nu = E_0 - \frac{E^2}{2mc^2}$$

The same amount of kinetic energy is transferred to the

3.

scattering nucleus. Thus the total energy difference is

$$\Delta E = E^2 / mc^2 \quad (3)$$

and the system is out of resonance by ΔE .

From electrodynamical theory, the resonant scattering cross-section is given by the Breit-Wigner relation²,

$$\sigma = g \frac{\lambda^2}{8\pi} \frac{\Gamma_1^2}{(E - E_0)^2 + (\Gamma/2)^2} \quad (4)$$

where $g = \frac{1+2J_e}{1+2J_g}$, J_e and J_g are the excited and ground state spins respectively, λ is the wavelength of the incident radiation, Γ_1 is the gamma ray transition probability for the absorption and re-emission transition and Γ is the total width of the level. The two possible modes of de-excitation for the 129-kev transition in Ir 191 are by emission of a gamma ray photon or by internal conversion. If N_e is the number of conversion electrons and N_γ is the number of photons emitted in the same time interval, the total internal conversion coefficient is

$$\alpha = \frac{N_e}{N_\gamma} = \frac{W_e}{W_\gamma} \quad (5)$$

where W_γ is the probability per unit time for emission of a photon and W_e is the probability per unit time that the same nuclear field will transfer its energy to any bound electron of its own atom. The total transition probability, i.e., the probability of the nucleus undergoing any transition is

$$W = W_e + W_\gamma = 1/\tau \quad (6)$$

where τ is the mean life of the transition. By the uncer-

4.

tainty principle, $\Gamma \tau \simeq \hbar$ and thus

$$\Gamma \simeq \Gamma_1 (1 + \alpha) \quad (7)$$

Combining equations (4) and (7), one obtains

$$\sigma = g \frac{\lambda^2}{8 \pi} \frac{\left(\frac{\Gamma}{1 + \alpha} \right)^2}{(E - E_0)^2 + (\Gamma/2)^2} \quad (8)$$

It may be observed that for a large ΔE in comparison with the level width Γ , the cross section becomes unobservably small. In practice, level widths of the order of 10^{-6} -ev and larger can be measured which correspond to mean lifetimes of the order of 10^{-9} seconds and shorter.

Several methods have been employed to restore the resonance condition; among them are the recoil due to preceding beta or gamma emission³, thermal motion by increasing the temperature of the source⁴, and through mechanical motion^{5,6}. All the methods require that the source be moving toward the scatterer with a velocity of the order of $u = E/mc$ so that the energy shift may be compensated by the Doppler-effect. For the 129-kev transition under study, $u = 2.2 \times 10^4$ cm/sec, a velocity which can be obtained at the edge of a high speed rotor.

An expression for the resonant scattering cross-section which takes into account the mechanical velocity u of the gamma source and the thermal velocities of the source and scattering nuclei has been derived by Moon^{5,6,7}. Consider that the thermal velocities of the nuclei are distributed

5.

as in a gas at a temperature T . Then the probability that a source and scattering nucleus have thermal velocity components that differ by v cm/sec in the gamma-ray direction is

$$P(v)dv = \sqrt{\frac{m}{4\pi KT}} e^{-\frac{mv^2}{4KT}} dv \quad (9)$$

Since the Doppler-effect adds an energy $(u + v)E/c$ to the gamma ray, $(E-E_0)$ is replaced by

$$\frac{E}{c}(u+v) - \frac{E^2}{mc^2}$$

in equation (8) and there results

$$\omega = g \frac{\lambda^2}{8\pi} \frac{\left(\frac{\Gamma}{1+\alpha}\right)^2}{\left(\frac{E}{c}\right)^2 \left(u+v - \frac{E}{mc}\right)^2 + \left(\frac{\Gamma}{2}\right)^2}$$

Multiplying by $P(v)$ and integrating,

$$\omega = g \frac{\lambda^2}{8\pi} \int_{-\infty}^{+\infty} \frac{P(v) \left(\frac{\Gamma}{1+\alpha}\right)^2 dv}{\left(\frac{E}{c}\right)^2 \left(u+v - \frac{E}{mc}\right)^2 + \left(\frac{\Gamma}{2}\right)^2}$$

The integrand has a sharp maximum around $v = E/(mc) - u$, and so little error results in replacing $P(v)$ by $P\left(\frac{E}{mc} - u\right)$.

Thus

$$\sigma = \frac{g \lambda^2 \Gamma^2}{8\pi(1+\alpha)^2} \sqrt{\frac{m}{4\pi K T}} e^{-\frac{m(u - \frac{E}{mc})^2}{4 K T}} \int_{-\infty}^{+\infty} \frac{dv}{\left(\frac{E}{c}\right)^2 \left(u+v - \frac{E}{mc}\right)^2 + \left(\frac{\Gamma}{2}\right)^2}$$

and so

$$\sigma = \frac{g h^2 c^2 \Gamma}{4 E^3 (1+\alpha)^2} \sqrt{\frac{m c^2}{4\pi K T}} e^{-\frac{m(u - \frac{E}{mc})^2}{4 K T}} \quad (10)$$

where λ is replaced by hc/E . At resonance, the rotor speed $u = E/mc$ and the resonant scattering cross section becomes

$$\sigma = \frac{g h^2 c^2 \Gamma}{4 E^3 (1+\alpha)^2} \sqrt{\frac{m c^2}{4\pi K T}} \quad (11)$$

For the 129-kev transition in Ir 191, $\alpha = 2.4^8$, $J_g = 5/2$, $J_g = 3/2$ and thus $g = 3/2$. Assuming a source and scatterer temperature of $300^\circ K$,

$$\sigma = 1.7 \times 10^{-19} \Gamma \text{ cm}^2/\text{ev} \quad (12)$$

Since Γ is of the order of 10^{-5} ev^1 , $\sigma \sim 1.7$ barns. For a rotor speed of $u = 0 \text{ cm/sec}$, the resonance scattering cross-section depends upon

$$e^{-\frac{m(u - \frac{E}{mc})^2}{4 K T}}$$

Calculating this factor using $T = 300^\circ$,

$$e^{-\frac{E^2}{mc^2 4 K T}} = .405$$

Thus for this off resonance condition, $\sigma = .69$ barns.

In the case for a source at a temperature T_1 moving toward a scatterer which is at a temperature $T_2 \neq T_1$, the average temperature is used in equation (10), i.e., T is replaced by $(T_1 + T_2)/2$. Thus by lowering the temperature of the scatterer, one should expect an enhancement of the resonance scattering cross-section as the rotor speed approaches the resonance velocity u .

Competing scattering processes which make the observation of the nuclear resonance fluorescence effect difficult are Compton scattering, Rayleigh scattering, Thomson scattering, and Delbruck scattering. For incident radiation of 129-kev, the quanta scattered inelastically at a scattering angle of 90° are of 103-kev and thus an energy selective gamma detector may be used to discriminate against them. Rayleigh scattering is due to the interaction of quanta with the bound electrons, Thomson scattering is due to the interaction of quanta with the nuclear charge and Delbruck scattering is the result of virtual pair production in the nuclear Coulomb field. Rayleigh scattering predominates in the X-ray region, the cross-section in this experiment being of the order of .34 barns. Thomson scattering is negligible at 129-kev in comparison to Rayleigh scattering while Delbruck scattering predominates at high energies.

The resonant scattering experiment on the 129-kev transition in Ir 191 is carried out by attaching Os 191 to a solid steel high speed rotor which can be spun to vel-

8.

ocities of 4.0×10^4 cm/sec, well above the 2.2×10^4 cm/sec required for the resonance condition. A scintillation counter is employed to detect the Rayleigh and resonance scattering from an iridium scatterer and the Rayleigh scattering from a lead scatterer. By choosing the lead scatterer to be of thickness

$$t_{Pb} = \frac{\rho_{Ir} Z_{Ir}}{\rho_{Pb} Z_{Pb}} t_{Ir} \quad (13)$$

where ρ is the density and z the atomic number of the element indicated by the subscript, a scattering cross-sectional area containing the same number of electrons is obtained for both scatterers. Thus the Rayleigh scattering will be approximately the same from both scatterers. One can then plot the ratio of iridium scattering to lead scattering versus the rotor speed to observe the resonance scattering effect. The data obtained is used to determine the resonant scattering cross-section which is used in equation (12) to determine the width of the level and subsequently the mean life of the nuclear state.

MAGNETICALLY SUSPENDED ROTOR AND ASSOCIATED APPARATUS**Historical:**

According to MacHattie⁹, speeds in excess of several thousand revolutions per second were first obtained in 1925 by Henroit and Huguenard who reported spinning a top-like conical rotor to 11,000 r.p.s. The rotor rode on a cushion of air in the conical cup of a stator, and was spun by a circular row of obliquely directed air jets. An improved form of this apparatus was first used by Moon⁶ to examine the resonance fluorescence effect in Hg 198. Later, Metzger¹⁰ employed an air supported and air driven rotor copied from a design of Beams¹¹ to study the resonance fluorescence in Hg 198, Pr 141 and Tl 203.

In 1941, MacHattie⁹ developed an apparatus for magnetically rotating rod and spherical rotors. MacHattie succeeded in driving a 3/32" diameter rotor to 110,000 r.p.s. and in exploding a 3/16" diameter rotor at 49,000 r.p.s. In 1946, Beams, Young and Moore¹², with improvements in MacHattie's apparatus, exploded rotors of 3.97 mm diameter at 77,000 r.p.s. and .795 mm diameter at 386,000 r.p.s. The maximum peripheral speed in all cases was about 10^5 cm/sec, well above the 2.2×10^4 cm/sec velocity required for the 129-kev transition in Ir 191.

Magnetic Suspension Apparatus:

The apparatus described here is patterned after a model being used at the General Motors Technical Center.¹³ The rotor R (Figure 2) is freely suspended in the glass vacuum chamber V by the axial magnetic field of the solenoid S. The horizontal stability of the rotor is maintained by the symmetrically diverging magnetic field of the solenoid and through viscous damping of both the solenoid's iron core C and the 1/8" diameter iron rod positioned beneath the rotor.

The vertical stability of the rotor is maintained by the sensing coil P which is part of the grid circuit of a partially neutralized tuned grid-tuned plate radiofrequency oscillator in the support circuit shown in Figure 3. Small variations in the height of the rotor change the "Q" of the grid circuit through the slight change in inductance and capacitance of the pick-up coil. Consider a virtual upward displacement of the rotor. This will increase the amplitude of oscillation in the grid circuit of the oscillator v_1 and thus in the plate circuit as the oscillator is partially neutralized. This results in an increase in potential across the cathode follower v_2 which causes a higher potential or error signal to be applied to the control grid of v_3 . The resulting decrease in potential on the grids of the parallel 5881's, v_4 , v_5 and v_6 causes a decrease in current through the support solenoid which restores the rotor to its original position through a decrease in the lifting

11.

FIGURE 2

MAGNETIC SUSPENSION APPARATUS

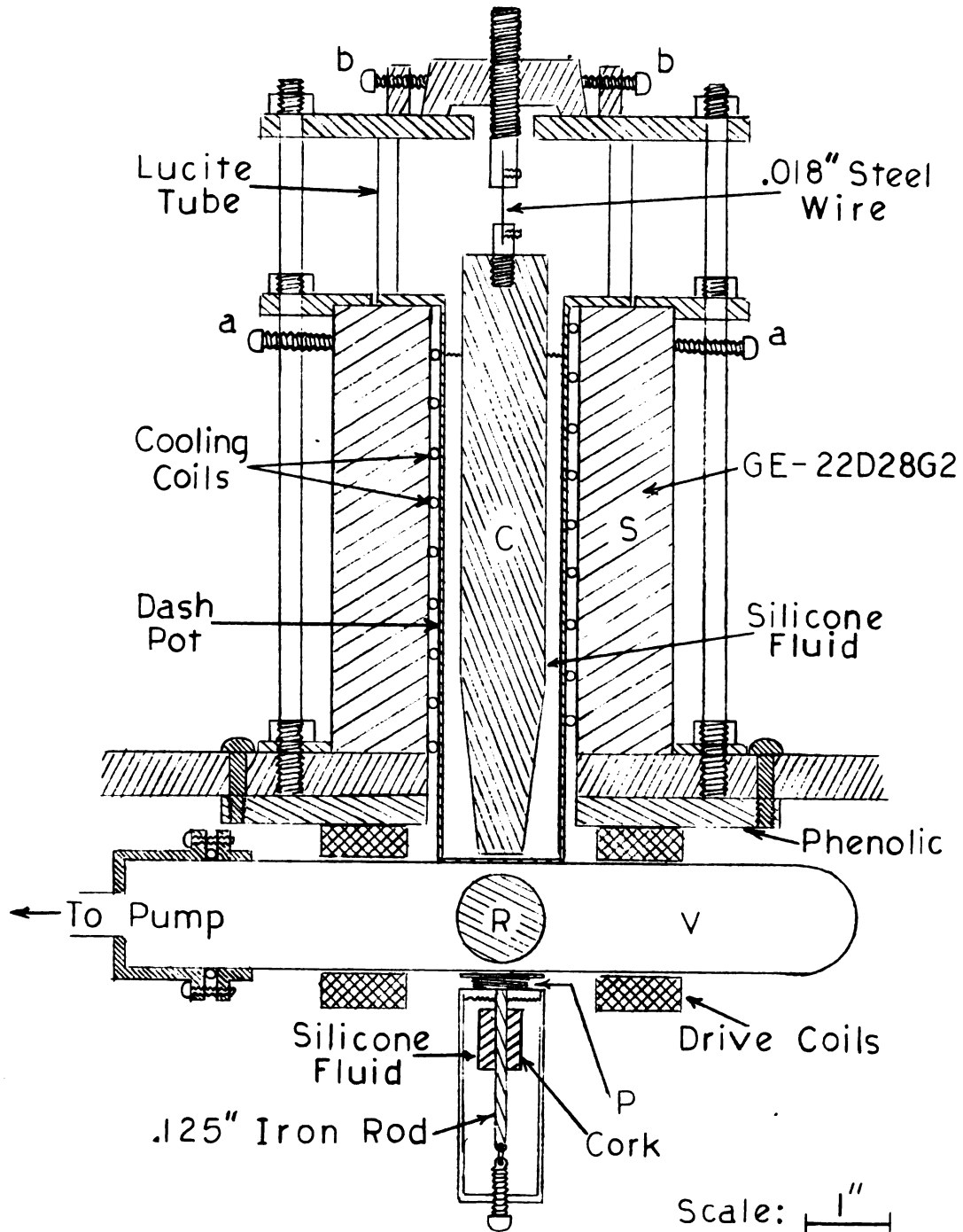
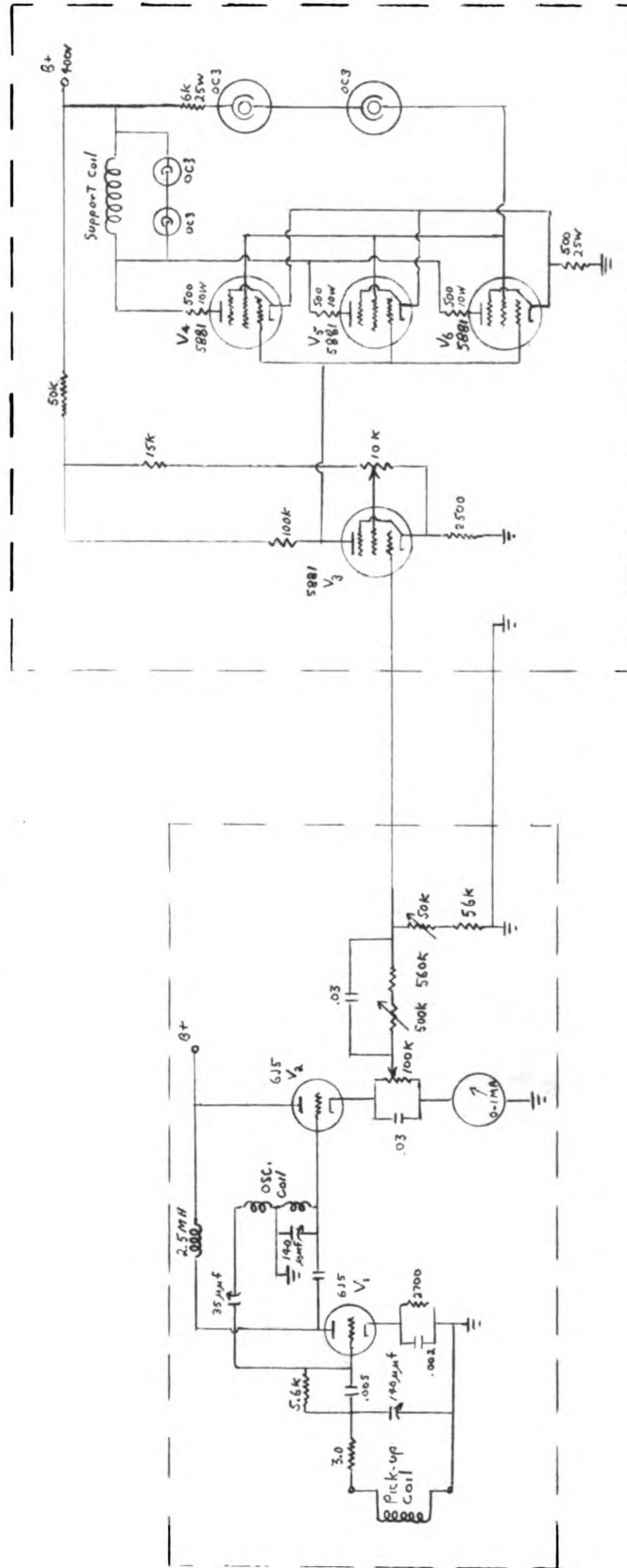
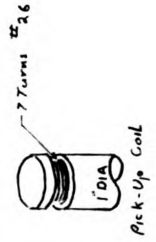
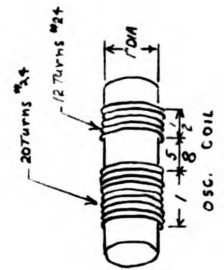


FIGURE 3



MAGNETIC SUSPENSION CIRCUIT



13.

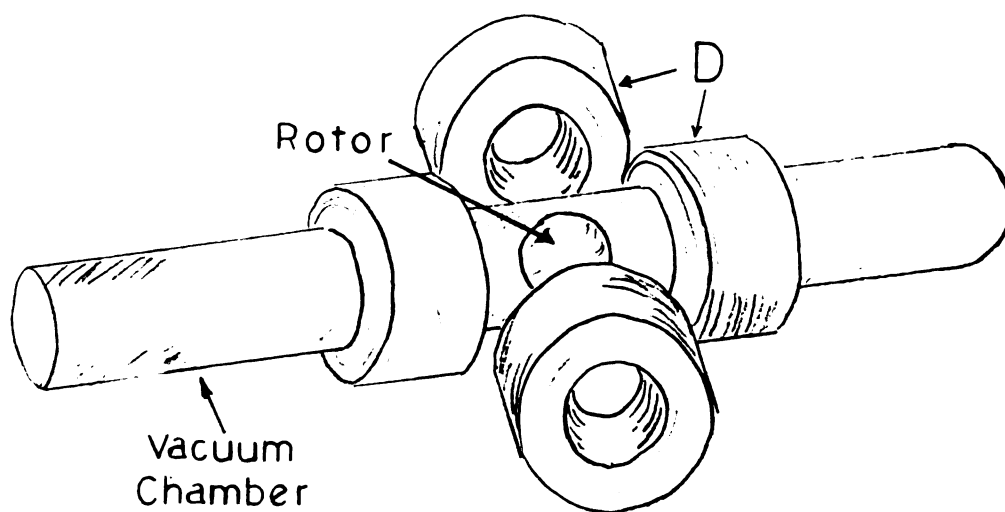
force. Any vertical oscillations (hunting) are eliminated by the differentiating circuit on the output of the cathode follower v_2 while the OC3 voltage regulators tend to stabilize the voltage across the solenoid.

The Magnetic Drive Circuit:

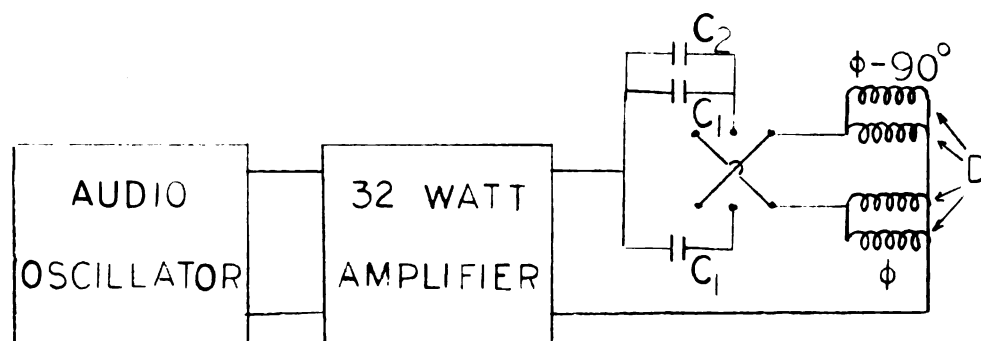
The rotor is spun by a rotating magnetic field produced by the four drive coils D shown in Figure 4a. These coils are mounted symmetrically about the rotor with opposite coils connected in parallel. The output of an audio oscillator is amplified by a 32 watt power amplifier and passed to a phase splitting circuit (Figure 4b). This circuit consists of two capacitors in parallel, each in series with a pair of drive coils, the capacity being determined by the desired driving frequency. The phase splitting is accomplished by making one of the resonant circuits more capacitive so that the currents in the two pairs of coils differ in phase by 90° . The currents in each pair are equalized by slightly detuning the resonant circuits, i.e., the frequency is adjusted to a point midway between the resonant frequencies of the two resonant circuits. Thus the solid steel rotor is actually the armature of an induction motor as the rotor is spun by the interaction of the eddy currents set up in the rotor with the rotating field. The "slip" is very high in starting the rotor but gradually decreases as the rotor accelerates.

FIGURE 4

MAGNETIC DRIVING CIRCUIT



(a)



(b)

15.

The coils each consist of 1000 turns of #26 Formex copper wire wound with an inside diameter of $5/4$ ", outside diameter of 2", a width of one inch and are of approximately 32 millihenrys inductance. The coils are mounted on a $3/8$ " thick Phenolic board as the peak to peak voltage across them is of the order of 1000 volts.

The Rotor:

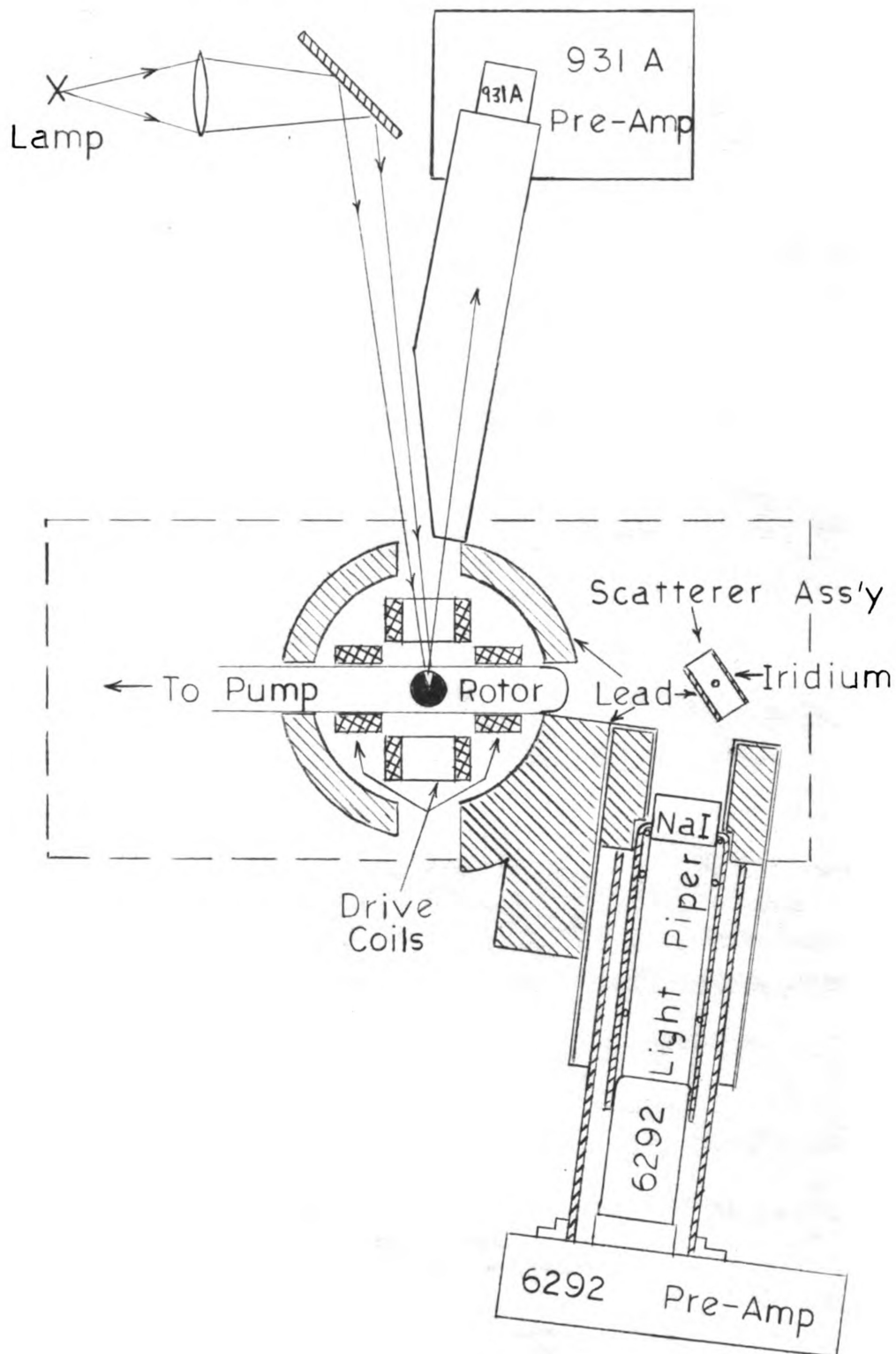
The rotor is prepared by grinding two diametrically opposite flats 15 mils deep on the rotor's surface through which will pass the axis of rotation. Two small grooves are placed diametrically opposite on the equator of the rotor, one groove to be used for the source, the other for a counterbalance. A 1" i.d., $33/32$ " o.d. x $1/8$ " wide ring turned from 7075-T6 aluminum is pressed over the equator of the rotor to hold the source and counterbalance in place in the afore mentioned grooves. The ring is of sufficient strength to be spun at a velocity of approximately 4.2×10^4 cm/sec without exploding (See Appendix).

Nuclear Counting Equipment:

A scintillation counter consisting of a NaI(Tl) crystal and a 6" length of 1.63" diameter lucite light piper mounted on a 6292 photomultiplier is used as the gamma detector (Figure 5). The light piper is employed to obtain a large distance between the 6292 photomultiplier and the suspension solenoid as the gain of the photomultiplier is adversely affected by the presence of a strong magnetic field.

16.

FIGURE 5
PHOTOMULTIPLIER ARRANGEMENT



Scale: 1"

The scatterer assembly consists of a .020" thick x 1.5" diameter iridium disk and a .037" thick x 1.5" diameter lead disk mounted on a .75" thick x 1.5" diameter aluminum rod. The thickness of the lead scatterer is chosen by equation (13). The scatterer assembly is mounted on the suspension apparatus so that in rotating the scatterer through 180° , the iridium or lead disk will face the source through the hole in one of the drive coils (See Figure 5). Three inches of lead is placed between the source and the NaI crystal of the gamma detector to reduce the intensity of the direct 129-kev radiation of 15 day Os 191 and the 880-kev radiation of 95 day Os 185 which are both present in the source. The 129-kev component is reduced by 10^{100} and the 880-kev component is reduced by 10^3 .

A gating system is employed so that the gamma detector is turned on only when the source is approaching the scatterer. In this manner, the signal to noise ratio is greater than that obtained if the source had been distributed about the circumference of the rotor. The gating is accomplished by darkening all of the rotor with black "Flo-Master"* ink except for a narrow vertical strip over the radioactive source. The light from an incandescent lamp (Figure 5) is focused on the spinning rotor and the resulting scattered light focused on a 931A photomultiplier. The signal is fed to a scaler where a frequency measurement of the rotor is

* Trademark, Cushman and Denison Mfg. Co., New York.

obtained. The shaped pulses of the frequency detecting scaler are fed to a gate circuit (Figure 6a) along with the output signal of the single channel pulse height analyzer of the gamma detector. The 6AH6 inverter tube (Figure 6c) of the gate circuit inverts the gamma signal which is then fed to one control grid of the 6BN6. The shaped pulse of the frequency detecting scaler is fed directly to the 2nd control grid of the 6BN6 which is biased to conduct only when both signals are present simultaneously, i.e., the square pulse drives the tube near conduction and any gamma signals incident during this time will cause the tube to conduct. The output of the gate is fed to a 2nd scaler which records the number of quanta scattered into the gamma detector while the source is approaching the scatterer. The width of the gate, i.e., the width of the shaped signal of the frequency detecting scaler, is controlled by the width of the reflecting line on the rotor.

FIGURE 6a
BLOCK DIAGRAM OF DETECTION SYSTEM

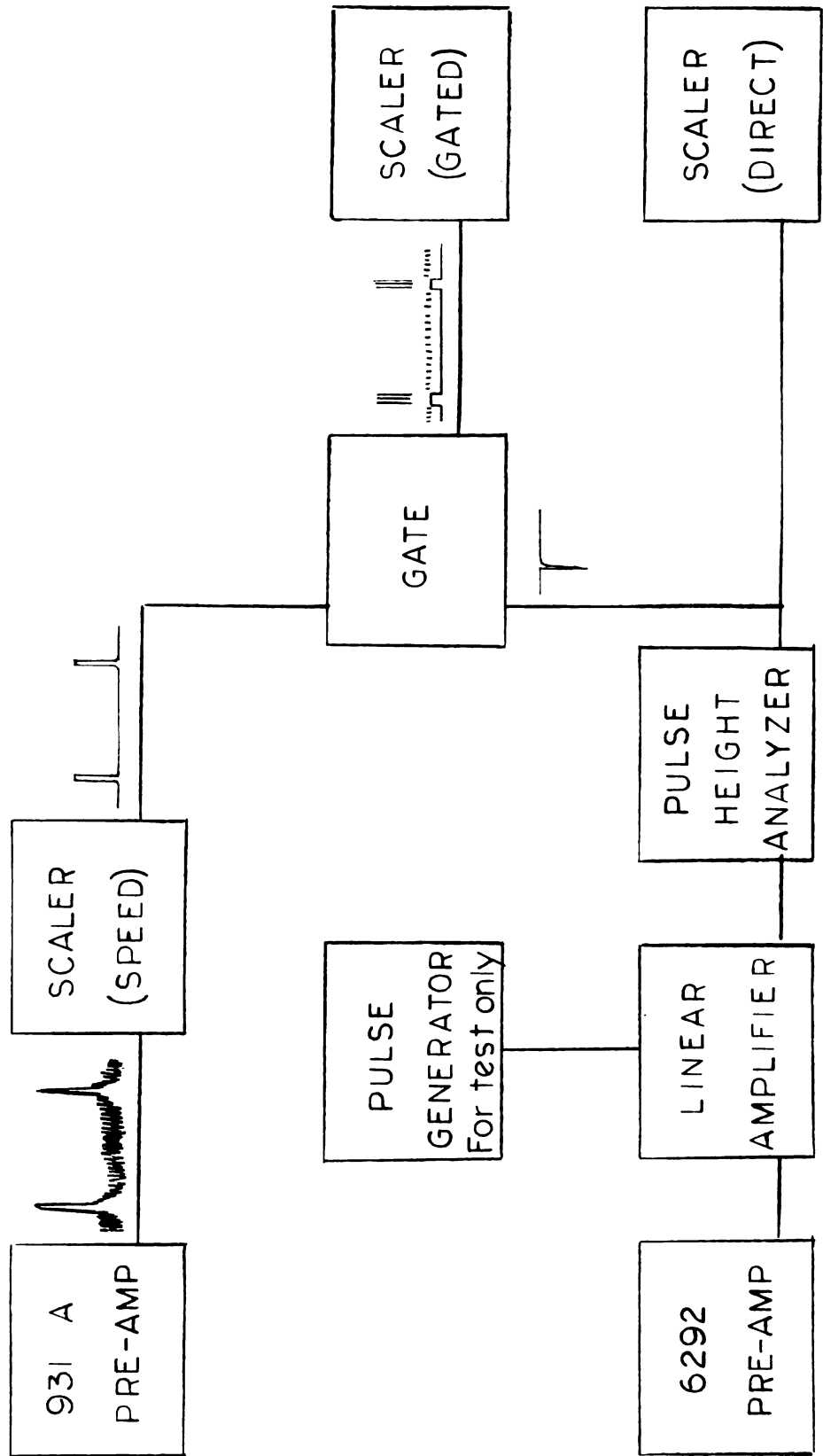


FIGURE 6b

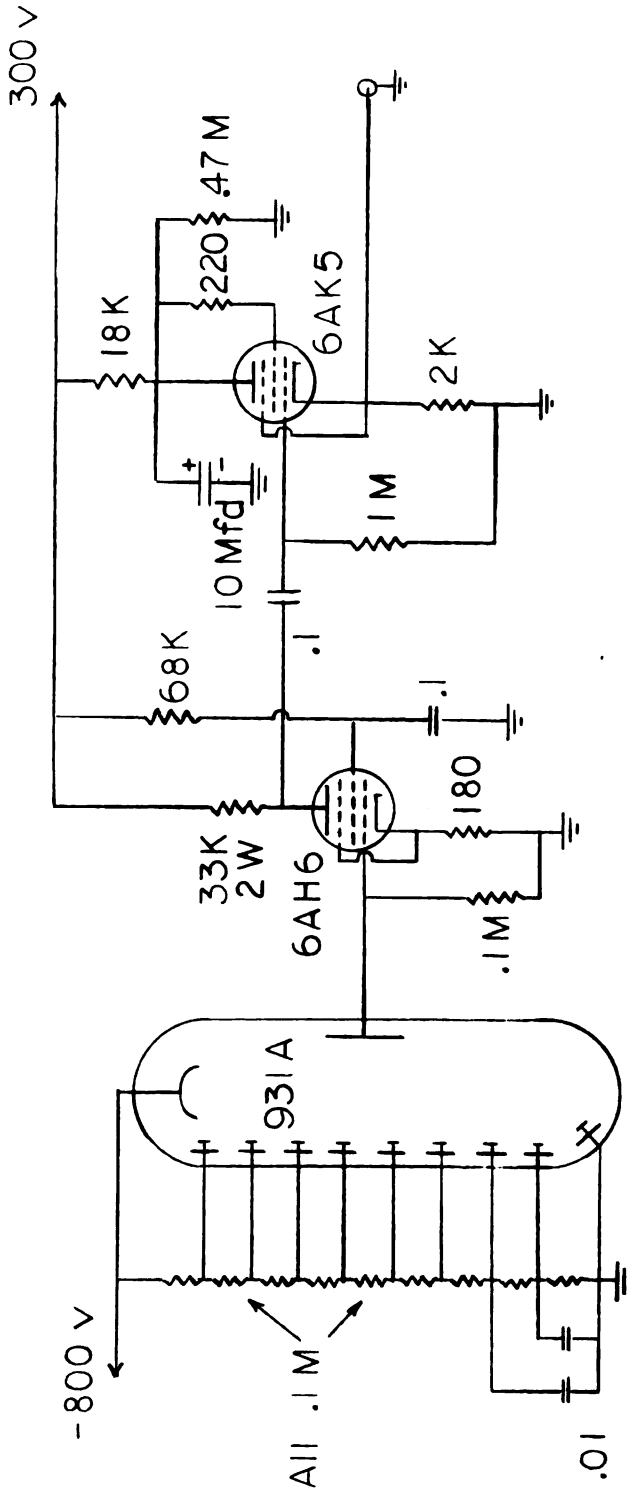
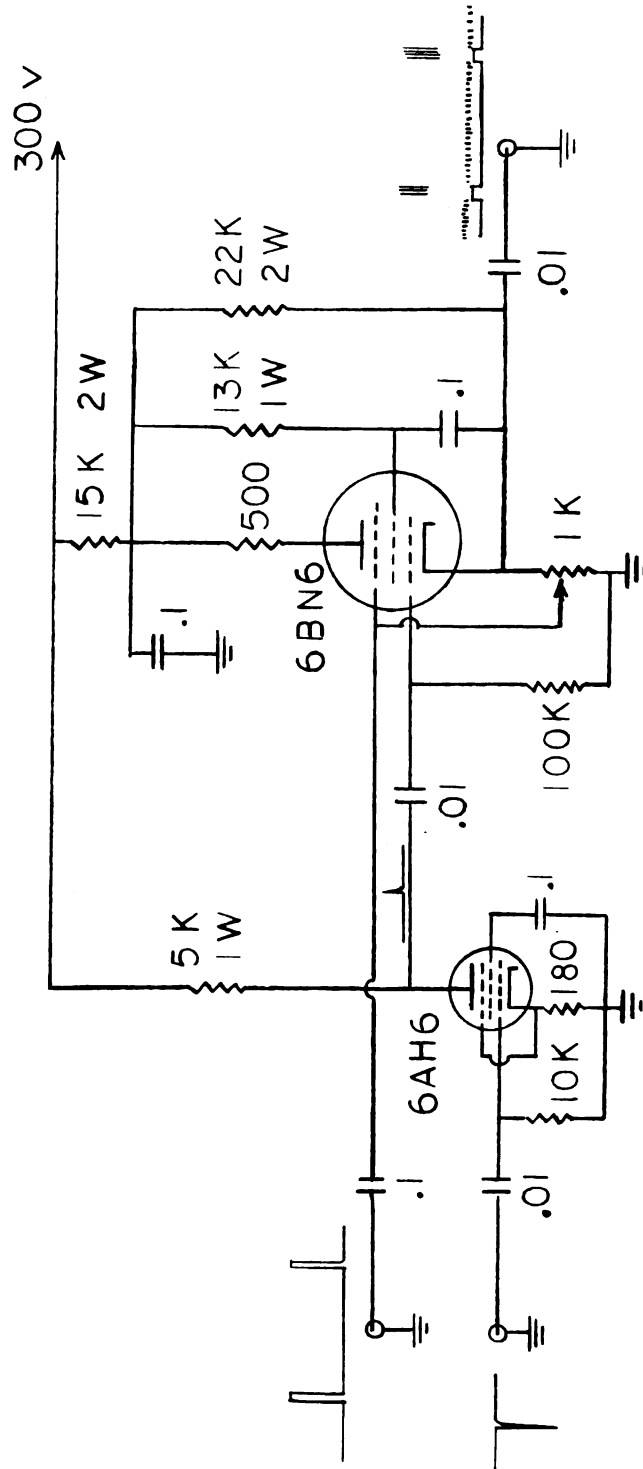


FIGURE 6c

GATE CIRCUIT



PERFORMANCE OF THE APPARATUS

Magnetic Suspension System:

In the early attempts to spin a one inch diameter steel rotor, considerable horizontal instability was encountered at frequencies around 1100-1200 r.p.s., i.e., the rotor would begin to precess and/or wobble back and forth until it was thrown from the magnetic field of the suspension solenoid. A number of causes contributing to this instability were found. Among these are:

1. Poor alignment of the magnetic axis of the solenoid with the gravitational field.
2. An unsymmetric iron core in the suspension solenoid.
3. Non-critical damping of the solenoid's iron core.

The reason that poor alignment should affect the stability is that under such circumstances, the iron core hangs in equilibrium between the force of gravity and the axial magnetic field of the solenoid. Any horizontal motion of the rotor is detected by the pick-up coil and results in a correction current being sent to the solenoid. The resultant variation in the magnetic field of the solenoid causes a small change in the position of the iron core which changes the position of the rotor. Thus the amplitude of oscillation increases. The system was aligned by hanging an 8" long x 1/8" diameter iron rod in the solenoid and observing

the motion of the rod while sharply varying the solenoid current. The solenoid was tilted by the adjustment screws a (Figure 2) and the rod was centered by the adjustment screws b at different vertical positions of the rod until no perceptible motion of the rod was observed.

The rotor's instability still persisted around 1600 r.p.s. and a check on the solenoid core showed it to be .007" out of round which indicated that the rotor had been spinning in an unsymmetric field. A new core was turned from cold rolled annealed Armco iron with a resultant increase in frequency of the rotor to 2700-2800 r.p.s.

Various viscosities of silicone damping fluids for the solenoid's iron core were obtained from 1000 c.s. and 10 c.s. Dow Corning 200 fluid. It was found that the rotor is the most stable for a viscosity of 100 c.s., as a viscosity of 98 c.s. gave stability to 3300 r.p.s., 100 c.s. gave stability to 3700 r.p.s. and 103 c.s. gave stability to 3070 r.p.s. Since 3700 r.p.s. corresponds to a peripheral velocity of 3.0×10^4 cm/sec, the resonance experiment on Ir 191 can be carried out. Further experimentation on the damping fluid will be necessary if other transitions more energetic than 129-kev are to be considered. The highest rotor frequency obtained was 5000 r.p.s. which was accomplished by adjusting the screws b so that the rotor would rub momentarily against the side of the vacuum chamber damping out the precessing motion.

The Magnetic Drive Circuit:

The rates of acceleration of the rotor in air for various driving frequencies were found as follows:

<u>Driving F.</u>	<u>Capacity C_1</u>	<u>Capacity C_2</u>	<u>Acceleration</u>
8800 ~	.02 Mfd	.0005 Mfd	0.55 r/sec ²
2500 ~	.25 Mfd	.015 Mfd	1.1 r/sec ²
1770 ~	.50 Mfd	.040 Mfd	1.5 r/sec ²

Thus for lower driving frequencies, a higher acceleration rate is obtained. In vacuum, ($\sim 10^{-4}$ mm-Hg) a driving frequency of 5000~ was employed ($C_1 = .05$ Mfd, $C_2 = .005$ Mfd) and an acceleration rate of 1.2 r/sec² was obtained, about the same as that for a 2500~ driving frequency in air.

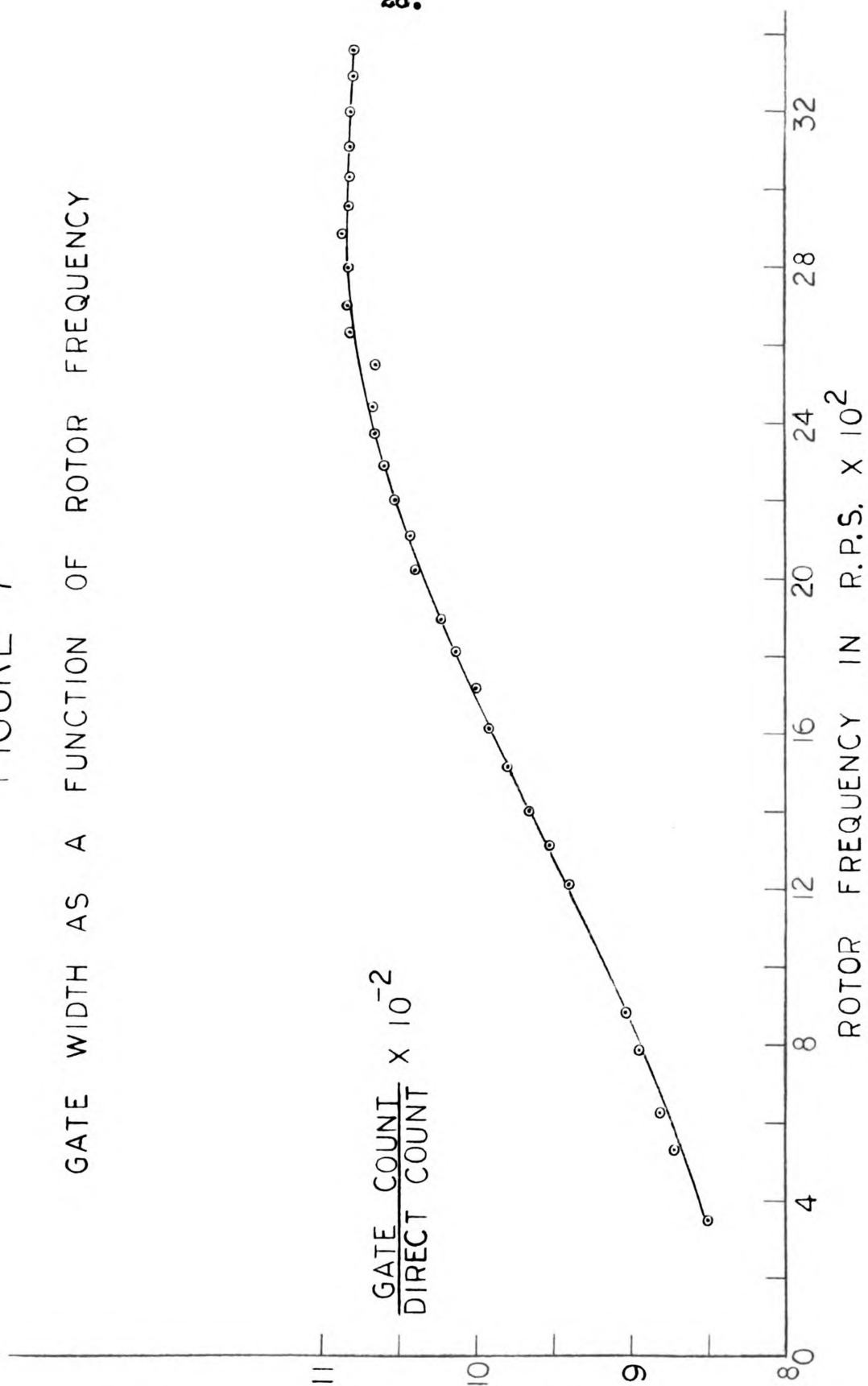
The "Flo-Master" ink is found to stay on the rotor very well during acceleration, however during deceleration, i.e., the drive circuit reversed, the ink begins to spray from the rotor in very tiny particles. This is believed to be due to heating of the rotor as the rotor is spinning at 3500 r.p.s. in one direction and the field in the opposite direction at 5000 r.p.s. and the resulting "slip" is very great. This heating effect should not bother when spinning the source as the rotor will be accelerated for short periods of time with data being taken while the rotor is coasting.

Nuclear Counting Equipment:

The gate width is measured by substituting a pulse generator for the gamma counter and recording the gated count and direct count at different velocities of the rotor (See Figure 6a). A plot of rotor frequency versus the ratio of the gated count to the direct count (Figure 7) indicates that the gate width increases as the rotor goes from zero to 2600 r.p.s. and remains constant as the rotor goes on up to 3400 r.p.s. The reason for the increasing gate width is that the risetime of the pulse from the rotor's timing mark varies inversely with speed and since the trigger circuit in the scaler relies on the signal's slope, the shaped pulse of the scaler will be of longer duration. Thus the gate will be open for longer periods of time at high rotor velocities. This effect will be taken into account when performing the resonance experiment on Ir 191.

FIGURE 7

GATE WIDTH AS A FUNCTION OF ROTOR FREQUENCY



APPENDIX

According to Timoshenko¹⁴, the stress in a thin ring which is rotated about its major axis of inertia is given by

$$s = \rho v^2 / g$$

where ρ is the mass density of the ring, v is its peripheral velocity and g is the acceleration of gravity. The tensile strength of 7075-T6 aluminum is 76×10^3 lbs/in², the yield strength is 67×10^3 lbs/in²,¹⁵ and the density is 10.27 lbs/in³. Employing the yield strength

$$v = 4.2 \times 10^4 \text{ cm/sec}$$

or a frequency of 5200 r.p.s. for a 1" diameter rotor.

BIBLIOGRAPHY

1. J. W. Mihelich, H. McKeown, M. Goldhaber, Phys. Rev. 92, 1450 (1954).
2. J. D. Jackson, Canad. Journ. Phys. 33, 575 (1955).
3. E. Pollard, D. Alburger, Phys. Rev. 74, 926 (1948).
4. K. G. Malmfors, Ark. f. Fysik 6, 49 (1952).
5. P. B. Moon, Proc. Phys. Soc. 63, 1189 (1950).
6. P. B. Moon, Proc. Phys. Soc. 64, 76 (1951).
7. K. G. Malmfors, Beta and Gamma Spectroscopy, edited by K. Siegbahn, (North-Holland Publishing Co., Amsterdam 1955) p. 521.
8. E. M. Bernstein, H. W. Lewis, Phys. Rev. 105, 1524 (1957).
9. L. E. MacHattie, Rev. Sci. Inst. 12, 429 (1941).
10. F. R. Metzger, J. Franklin Inst. 261, 219 (1956).
11. J. W. Beams, Rev. Mod. Phys. 10, 245 (1938).
12. J. W. Beams, J. L. Young III, J. W. Moore, J. Appl. Phys. 17, 886 (1946).
13. Private communication with Mr. Wayne Chapman of the General Motors Technical Center, Warren, Michigan.
14. S. Timoshenko and G. MacCullough, Elements of Strength of Materials, (D. Van Nostrand Co., Inc. 1940) p. 23.
15. Central Steel, Handbook of Central Steel and Wire Co., 1955-1956, p. 325.

PHYSICS-MATH LIB.

MICHIGAN STATE UNIV. LIBRARIES



31293016875902